Dynamics of Water Associated with Lithium Ions Distributed in Polyethylene Oxide

Zhe Zhang,[1,2] Michael Ohl,[2] Souleymane O. Diallo,[3] Niina H. Jalarvo,[2,4] Kunlun Hong,[5] Youngkyu Han,[1] Gregory S. Smith,[1] and Changwoo Do[1,*]

[1]*Biology and Soft-Matter Division, Oak Ridge National Laboratory, Oak Ridge, Tennessee 37831, USA*

[2]*Forschungszentrum Jülich, Jülich Center for Neutron Science, Outstation at the Spallation Neutron Source (SNS), Oak Ridge National Laboratory, Oak Ridge, Tennessee 37831, USA*

[3]*Quantum Condensed Matter Division, Oak Ridge National Laboratory, Oak Ridge, Tennessee 37831, USA*

[4]*Chemical and Engineering Materials Division, Neutron Sciences Directorate, Oak Ridge National Laboratory, Oak Ridge, Tennessee 37831, USA*

[5]*Center For Nanophase Materials Sciences Division, Oak Ridge National Laboratory, Oak Ridge, Tennessee 37831, USA*

(Received 19 February 2015; revised manuscript received 12 September 2015; published 3 November 2015)

The dynamics of water in polyethylene oxide (PEO)/LiCl solution has been studied with quasielastic neutron scattering experiments and molecular dynamics (MD) simulations. Two different time scales of water diffusion representing interfacial water and bulk water dynamics have been identified. The measured diffusion coefficient of interfacial water remained 5–10 times smaller than that of bulk water, but both were slowed by approximately 50% in the presence of Li^+. Detailed analysis of MD trajectories suggests that Li^+ is favorably found at the surface of the hydration layer, and the probability to find the caged Li^+ configuration formed by the PEO is lower than for the noncaged $Li^+ - PEO$ configuration. In both configurations, however, the slowing down of water molecules is driven by reorienting water molecules and creating water-Li^+ hydration complexes. Performing the MD simulation with different ions (Na^+ and K^+) revealed that smaller ionic radius of the ions is a key factor in disrupting the formation of PEO cages by allowing spaces for water molecules to come in between the ion and PEO.

DOI: 10.1103/PhysRevLett.115.198301 PACS numbers: 82.47.Aa, 07.05.Tp, 28.20.Cz

Water and water-containing systems are ubiquitous in nature. Water plays an essential role in many physical processes [1,2] and chemical reactions [3,4], as well as biological properties [5–9]. Generally, water can be categorized into two populations in water-containing systems: bulk water and interfacial water [10,11]. The bulk water molecules exist away from the solute or the interfaces where atomistic and molecular interactions with them can be ignored [11,12], while the interfacial water molecules are usually found near the solute or interfaces having properties different from bulk water [13–19]. The interfacial water molecules often demonstrate extraordinary structural and dynamical properties compared to those of the bulk water molecules [14,18,19], and efforts are still being made to understand the structure and dynamics of interfacial water under various confinement [20].

The role of water in polymeric systems with salts has long been investigated in soft matter research for both fundamental science and application development. The properties of polymers and ions in these systems have shown strong dependencies on the structure and dynamics of interfacial water (or hydration water) molecules. For example, the forward rate of proton hopping in Nafion is known to be determined by the orientational dynamics of water near the polymer [21]. In solid polymer electrolyte batteries [22–24] based on polyethylene oxide (PEO) and lithium, it has been reported that hydrating PEO increases the conductivity by as much as 1000 times that of the typical binary mixture of PEO/lithium salts [25,26]. Such enhancement was attributed to water absorption, which increases the mobility of PEO chains, producing more free mobile ions by reducing the coordination between PEO and cations [26,27]. Therefore, understanding the insight of water dynamics associated with Li^+ distribution in aqueous PEO/Li^+ solution can aid in the potential development of lithium batteries with high conductivity and capacity. Furthermore, studying the interplay among water, salts, and polymers will result in an important guidance for the desired functional materials.

Water dynamics is playing a critical role in the function of materials, which can be seen directly from the above examples, however, most of the focus has been given to the influence of water on the behaviors of polymers and ions, and much less attention has been given to the structure and dynamics of water itself, i.e., what is the effect on water dynamics from polymers and ions? In order to answer this question, a detailed analysis of water dynamics associated with the microstructure of the polymer-ion-water complex is needed. Among polymers, PEO has important applications for medical uses [28–31] in human or animal bodies that include an abundance of water and ions, as well as to energy storage applications. Therefore, the PEO-ion-water complex has been chosen as a model system to study water dynamics influenced by surrounding polymers and ions.

Neutron scattering and molecular dynamics (MD) simulation have been widely used to study water dynamics in

the past [32–34]. The energy of neutrons and the large incoherent scattering cross section of hydrogen, made quasielastic neutron scattering a powerful tool for accessing the dynamics of water in sub ps to ns time scales. By having similar length and time scales, atomistic MD simulation is a complementary tool to neutron scattering to obtain experimentally inaccessible information such as atom positions and dynamics [24,35,36]. Here, we use quasielastic neutron scattering (QENS) and MD simulations to study a PEO/water mixture (wt % = 50%) with and without lithium salts (LiCl) (Molar ratio $EO:Li^+ = 10:1$).

In this study, water can be clearly categorized into bulk water and interfacial water by the boundary of the hydration layer at $R = 4$ Å, where R is the distance between the water molecule and PEO chains (see Supplemental Material [37], which includes Refs. [12,38–57]). Recent studies by broadband dielectric spectroscopy, nuclear magnetic resonance (NMR), and MD simulation have shown bulk water and interfacial water have significant heterogeneity [58–62], especially the alpha and beta relaxation process. The beta-relaxation process is a local process which can be observed below the glass transition temperature ($T_g < 175$ K [58]), and usually merges with the alpha-relaxation process above T_g [58,63]. The QENS experiment was taken at $T = 300$ K in this study, which is much higher than T_g; thus, only alpha relaxation is visible in the experiment. Therefore, two dynamic scales, representing bulk and interfacial water, in both QENS and MD simulation have been considered by two Lorentzian functions when modeling the dynamic structure factor $S(q, E)$, where E is the energy in Fourier transform [37] and q is the wave vector. Following the approaches by Barnes and Leyte [46], the dynamic structure factor at each q is given as

$$S(q,E) = B \times \left[(1-f) \times \frac{\Gamma_1}{\Gamma_1^2 + E^2} + f \times \frac{\Gamma_2}{\Gamma_2^2 + E^2} \right], \quad (1)$$

where Γ_1 and Γ_2 are the widths of the Lorentzian curves representing the dynamics for bulk and interfacial water, respectively. f is the fraction of interfacial water. In general, the dynamics of bulk water molecules are described by combinations of rotational diffusion and translational diffusion processes [54,64]. However, within the q range and energy range explored by BASiS (0.3 Å$^{-1} < q < 1.1$ Å^{-1}, -115 μeV $< E < 115$ μeV), the rotational diffusion can be neglected and, therefore, the bulk water diffusion process can be approximated by pure translational diffusion, which can be given by $\Gamma_1 = D_1 q^2$, where D_1 is the q-independent diffusion coefficient. Thus $S(q, E)$ with different q values were simultaneously fit with a single D_1. Examples ($q = 0.5$ Å^{-1}) of successful data fitting results are shown in Fig. 1(a) (from QENS experiments) and Fig. 1(b) (from MD simulation), respectively (the detailed fitting procedures and fitting results can be found in the Supplemental Material [37]). Fitting with two Lorentzian functions

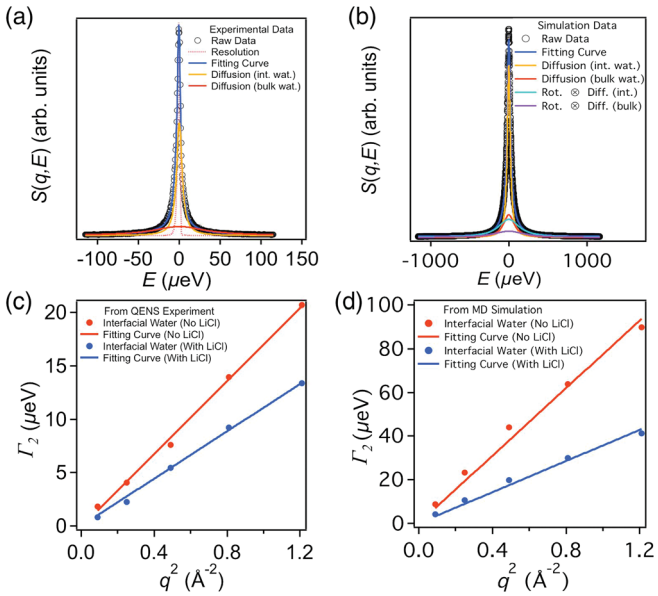

FIG. 1 (color). Comparison of the QENS experiment and MD simulation. (a) Data fitting of the QENS experiment (PEO/water solution without LiCl at $q = 0.5$ Å^{-1}). (b) Data fitting of the MD simulation (PEO/water solution without LiCl at $q = 0.5$ Å^{-1}) (compared to the other two components, the rotational component is very flat, in order to give a better representation, the amplitude of the peak was zoomed in by ×10.). (c) Linear fitting of Γ_2 vs q^2 (interfacial water) obtained from the QENS experiment. (d) Linear fitting of Γ_2 vs q^2 (interfacial water) obtained from MD simulation.

[Eq. (1)] resulted in excellent agreement with both the QENS data and the MD simulation data as shown in these figures, supporting the existence of two dynamic processes. The range of the energy axis of MD simulation in Fig. 1(b) is different from that of the QENS experiment, because the MD simulation explored the larger energy spectrum where the broadening due to the rotational motion of water molecules can also be seen [Fig. 1(b), green and purple lines]. The rotational motion of water molecules was modeled with an infinite stretched exponential series when calculating the intermediate scattering function, and, in order to reduce the calculation time, only the first two terms of the series were considered in the fitting procedure [37,53,54]. The fitted Γ_2 using Eq. (1) are shown in Figs. 1(c) and 1(d) for selected q values. A dramatic slowing down of the dynamic process by half is clearly observed when LiCl was added to the system from both the experiments and simulations. Γ_2 is also found to follow $\Gamma_2 = D_2 q^2$ in both PEO/water and PEO/water/LiCl systems, suggesting that the diffusion process can be characterized by the q-independent translational diffusion coefficient D_2. This indicates that the presence of LiCl only influences the dynamics scales but does not change the fundamental characters of the motion. The diffusion coefficients estimated from the fitting are summarized in the Supplemental Material [37].

The diffusion coefficients of the bulk water obtained from the QENS and MD simulation agrees with known values from the literature. However, the values from MD simulation is about twice as large as the experimental value [65–68], where such quantitative discrepancy is generally understood by the fact that the MD simulation is using an effective interaction potential to describe the dynamic properties of the system, which is a simplified model, while the QENS experiments measure the details of the molecular interaction directly in the solution [69]. Borodin and collaborators [64] reported the concentration dependence of water dynamics in PEO/water solution by MD simulation. The diffusion coefficient of interfacial water which was estimated to be 1×10^{-5} cm^2/s at 50 wt% PEO, is consistent with the number we obtained from our MD simulation analysis. From MD simulation, the fraction of interfacial water molecules can be estimated by counting the number of water molecules within the hydration layer defined by the distance 4 Å [37]. On average, 68% of water molecules are found to be interfacial water based on our MD trajectory analysis. This fraction is very close to the fraction of interfacial water ($f = 73\%$) obtained from QENS experiment, again suggesting that MD simulation and QENS experiment are in good agreement.

In bulk, the reorientation of water molecules toward Li^+ and the formation of hydration complexes (Li^+-water) [37] are responsible for the dynamic slow down of water molecules as well as the increased viscosity, which has been noted by Stirnemann and co-workers in their study on water-ion solutions [57]. The Li^+, however, does not remain in bulk or near interfaces of polymers but changes its position over time, influencing the dynamics of both the bulk and the interfacial water molecules. For example, distances from PEO to the selected Li^+ ions have been traced and representative data are shown in Fig. 2(a). It is interesting to note that whenever Li^+ ions are at the closest distance from PEO (~2 Å), they stay longer than when they are away from PEO. For example, Li 617 (orange) remains at a distance of 2 Å for almost 1 ns at the beginning, then goes to the bulk region. Based on the fluctuations of the distance from 1 to 3.5 ns, it is also clear that Li 617 moves in and out of the hydration layer ($R \sim 4$ Å) quite frequently. When its distance becomes ~2 Å again at around 4 ns, a brief moment of constant distance is again observed. Similar observations are commonly found in other Li^+ ions in the same plot. Li 616 exhibits a longer residing time at the closest distance and fluctuates between the hydration layer and the bulk region. Li 630 mostly stays under the hydration layer, while Li 618 shows more dramatic motions moving in and out of the hydration boundaries. Three distinctive types of motion can be identified from this observation. First, when Li^+ ions are at the closest distance from PEO, they are trapped longer than usual. Second, Li^+ tends to spend a significant amount of time at a distance of 4 Å, which is the hydration layer boundary. Third, Li^+ ions

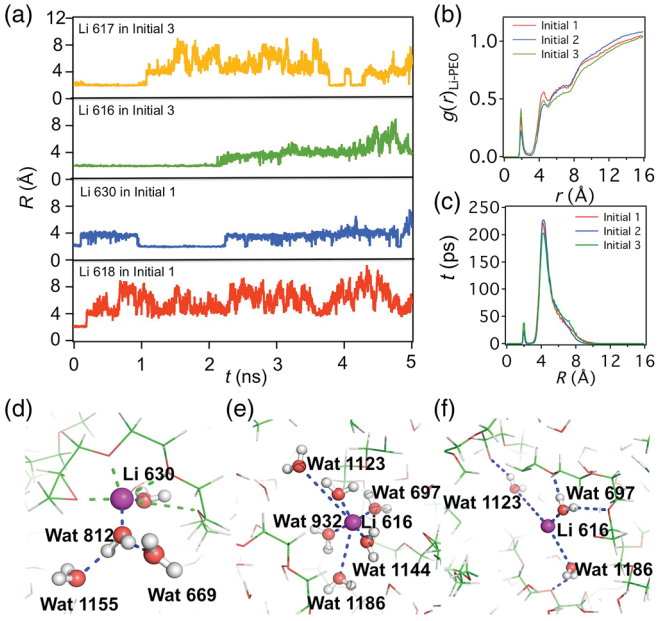

FIG. 2 (color). Li^+ distribution with respect to the distance to PEO. (a) Distances of four Li^+ from PEO during simulation. $R = 4$ Å is the boundary of the hydration layer. Three different initial structures (initial 1, initial 2, and initial 3) have been used for the MD simulation to ensure the validity of the simulation results. (b) Pair distribution function of Li^+ with the respect to PEO. (c) The distribution of the total time that Li^+ spends at various distances from PEO. (d)–(f) Green and red lines represent PEO (green, carbon atoms; red, oxygen atoms); purple ball represents Li^+; dashed lines indicate the interaction between two atoms (green, interaction between Li^+ and PEO; blue, interactions involved in water, i.e., water and PEO, water and Li^+, or water and water). (d) A snapshot ($t = 1500$ ps) of the PEO-Li^+_{630}-water complex when the Li^+ was trapped by PEO. (e)-(f) A snapshot ($t = 3825$ ps) of the PEO-Li^+_{616}-water complex when the Li^+ (Li 616) was located at the boundary of the hydration layer. (e) and (f) The same complex viewed from different angles, in particular, (f) is aimed to indicate water 697, water 1123, and water 1186 within the hydration layer.

move in and out of the hydration boundary, therefore interacting with both the interfacial water molecules and the bulk water molecules. These characteristics are also found in statistically averaged quantities like a pair distribution function of Li^+ with respect of PEO, $g(r)_{\text{Li-PEO}}$ [Fig. 2(b)]. The peak at 2 Å corresponds to the trapped Li^+, and the broader peak at 4 Å represents Li^+ ions that are more frequently found near the hydration layer boundaries. The distribution of total time that Li^+ ions spend at various distances from PEO ($t - R$ distribution) is also calculated, and shows that Li^+ ions spend most of their time near the hydration layer boundary which is around 4 Å. The preferential appearance at short distances (2 Å) is observed clearly as well, suggesting caging by PEO as in the pair distribution function. [Fig. 2(c)].

The representative spatial configurations for trapped Li^+ ions and the Li^+ ions at the hydration layer boundaries are

captured in the snapshots shown in Figs. 2(d)–2(f). The trapped Li^+ in fact shows the Li^+ ions caged by the PEO due to the strong interaction between Li^+ and the oxygen atoms of PEO [24,70,71]. The segmental motion of PEO, which is determined by the solvent viscosity and temperature, promotes a longer residing time for the caged configuration [24]. Although Li^+ is caged [Fig. 2(d)], it still influences nearby water molecules such as water 812 (first nearest neighbor), water 1155, and water 669 (second nearest neighbor) contributing to the overall dynamics of water. When Li^+ is at the hydration layer boundary [Figs. 2(e)–2(f)], interaction of Li^+ with both of the interfacial water molecules (water 697, water 1123, and water 1186) and the bulk water molecules (water 932 and water 1144) is observed. The interfacial water molecules that are strongly bounded by the PEO contribute to form Li^+-water complexes resulting in Li^+ distribution bounded to the hydration layer. This microstructure of the Li^+-water complex is practically the same as that in bulk, which indicates that the dynamic slowing-down process for interfacial water, in principle, is very similar to that in the bulk region.

Generally speaking, monovalent cations could have distinct behavior due to their size [72,73]. In order to better understand what influences the relative probability of Li^+ being in the caged configuration or the hydration layer boundaries, additional simulations with different ions of the same charge have been performed. After the same series of simulations with Na^+ and K^+ replacing Li^+, the $t-R$ distributions were calculated [Figs. 3(a) and 3(b)]. It is very clear that in aqueous PEO/NaCl and PEO/KCl solutions, the ion-caging effect is much stronger and dominant than in PEO/LiCl solution. While the $t-R$ distribution does not differentiate stationary ions and moving ions explicitly, the relative comparison of the amplitude of this distribution still enables comparison of the relative trapping time of ions. The $t-R$ distribution suggests that on average Na^+ ion was trapped for ~380 ps total, while K^+ ions spent longer time (>400 ps total) at distance $R = 2$ Å [Figs. 3(a) and 3(b)]. By inspecting individual ions trajectory, it was also confirmed that K^+ ions stay indeed longer in the cages ($R = 2$ Å) [insets of Figs. 3(a) and 3(b)]. While these ions were also observed near the hydration layer boundaries as indicated by the peaks around 4 Å, a caged configuration is found to be much more dominant compared to the Li^+ case. The number of ions that has ever been captured (based on the distance, $R \leq 3$ Å) by more than 3 EO monomers during 5 ns simulation can be directly counted. It turns out that more than half (13) K+ ions out of 24 have been caged, while the number of caged ions become fewer for smaller ions, i.e., 9 and 2 for Na+ and Li+, respectively [37]. The total time that these ions spend while being caged is also found to be the longest for the K^+ ions (4.4 ns) and shortest for the Li^+ (0.64 ns) [37]. These estimations indicate that the ions with large ionic radius not only form the cages

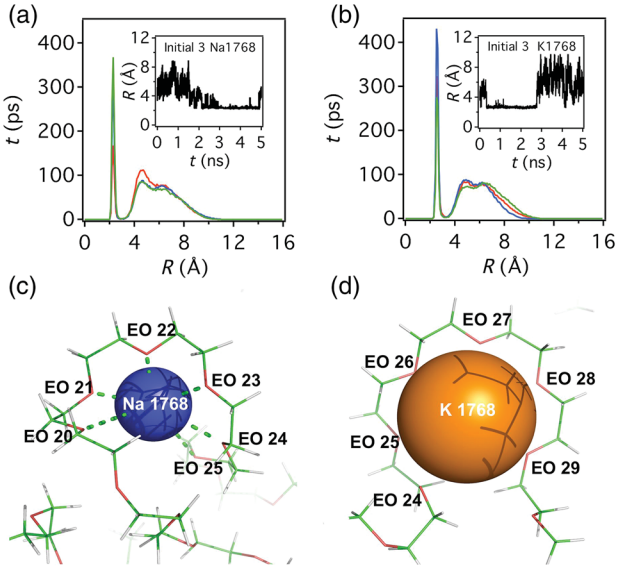

FIG. 3 (color). Trapping Na^+ and K^+. (a) Temporal distribution of Na^+ ions along with their distance from PEO chains: red, initial 1; blue, initial 2; and green, initial 3. The inset represents an example (Na 1768 from initial 3). (b) Temporal distribution of K^+ ions along with their distance from PEO chains: red, initial 1; blue, initial 2; and green, initial 3. The inset represents an example (K 1768 from Initial 3). (c) A snapshot of Na 1768 (blue ball) from initial 3 at $t = 4000$ ps; PEO was represented with green and red lines and the dashed line represents the interaction between Na 1768 and residues in PEO ("EO" represents PEO residue: ethylene oxide; and the number was the residue ID). (d) A snapshot of K 1768 (orange ball) from initial 3 at $t = 1500$ ps. PEO is represented with green and red lines. The interaction dashed line was not shown due to the small space inside of the cage.

easily but also stay within the cages longer than the smaller ions. By examining the caging structure for Na^+ and K^+ represented by the ionic radii as shown in Figs. 3(c) and 3(d), we found that less volume is available for water molecules to come in between the ions and the surrounding polymers. Water is competing with PEO for ions, thus is playing an important role in breaking PEO cages, which can be seen from the fact that the number of water molecules surrounding caged ions is less than that of noncaged ions [37]. We believe that as the size of the ions become larger, it becomes more difficult for the water molecules to penetrate between the ions and PEO, reducing the chances of disrupting the ion-PEO interactions and slowing down the segmental motions of PEO. Thus, it becomes difficult to release ions from the cages and slows down ion transportation. These observations agree with the well-known fact that Li^+, among many other ions, produces the best ionic conductivities in PEO-based solid polymer electrolyte batteries [25]. In addition, our simulation also confirms that the cage opening and closing plays an essential role in assisting ion transportations in polymer electrolytes [24].

In aqueous PEO-LiCl solution, we observe that the water dynamics both in bulk and at the interfaces of PEO were dramatically slowed down by almost half with both the QENS experiment and MD simulation. A detailed investigation of the MD trajectories reveals that Li^+ ions are more frequently found in the hydration layer boundaries interacting with both of the interfacial water molecules and the bulk water molecules. By replacing Li^+ with Na^+ or K^+, the caged ion-PEO complex became a major microstructure due to the bigger ionic radius that prevents water molecules from coming in for disruption of the cage conformation. To our knowledge, this is the first study providing the detailed processes of dynamics changes of water molecules influenced by ions both in bulk and near the interfaces. The revealed interplay of water molecules and ion-PEO complex structures will provide valuable insights in designing polymer-based ion batteries.

The research at Oak Ridge National Laboratory's Spallation Neutron Source was sponsored by the Scientific User Facilities Division, Office of Basic Energy Sciences, U.S. Department of Energy. Z. Z. gratefully acknowledges financial support from Jülich Center for Neutron Science, Research center Jülich. The authors gratefully thank Dr. E. Mamontov and Dr. W.-R. Chen for their input and valuable discussions.

doc1@ornl.gov

[1] J. C. Palmer, F. Martelli, Y. Liu, R. Car, A. Z. Panagiotopoulos, and P. G. Debenedetti, Nature (London) **510**, 385 (2014).
[2] E. B. Moore and V. Molinero, Nature (London) **479**, 506 (2011).
[3] M. Maroncelli, J. Macinnis, and G. R. Fleming, Science **243**, 1674 (1989).
[4] I. Ohmine and S. Saito, Acc. Chem. Res. **32**, 741 (1999).
[5] R. H. Zhou, X. H. Huang, C. J. Margulis, and B. J. Berne, Science **305**, 1605 (2004).
[6] F. T. Burling, W. I. Weis, K. M. Flaherty, and A. T. Brunger, Science **271**, 72 (1996).
[7] J. P. Lin, I. A. Balabin, and D. N. Beratan, Science **310**, 1311 (2005).
[8] J. Tian and A. E. Garcia, J. Am. Chem. Soc. **133**, 15157 (2011).
[9] J. A. Lemkul and D. R. Bevan, J. Phys. Chem. B **114**, 1652 (2010).
[10] M. F. Kropman and H. J. Bakker, Science **291**, 2118 (2001).
[11] J. Israelachvili and H. Wennerstrom, Nature (London) **379**, 219 (1996).
[12] B. Bagchi, Chem. Rev. **105**, 3197 (2005).
[13] J. Song, J. Franck, P. Pincus, M. W. Kim, and S. Han, J. Am. Chem. Soc. **136**, 2642 (2014).
[14] T. Shikata, M. Okuzono, and N. Sugimoto, Macromolecules **46**, 1956 (2013).
[15] J. H. Tian and A. E. Garcia, Biophys. J. **96**, L57 (2009).
[16] J. H. Tian and A. E. Garcia, J. Chem. Phys. **134** (2011).
[17] G. Hummer, J. C. Rasaiah, and J. P. Noworyta, Nature (London) **414**, 188 (2001).
[18] J. K. Holt, H. G. Park, Y. Wang, M. Stadermann, A. B. Artyukhin, C. P. Grigoropoulos, A. Noy, and O. Bakajin, Science **312**, 1034 (2006).
[19] D. Z. Liu, Y. Zhang, C. C. Chen, C. Y. Mou, P. H. Poole, and S. H. Chen, Proc. Natl. Acad. Sci. U.S.A. **104**, 9570 (2007).
[20] A. Paciaroni, M. Casciola, E. Cornicchi, M. Marconi, G. Onori, M. Pica, R. Narducci, A. De Francesco, and A. Orecchini, J. Phys. Condens. Matter **18**, S2029 (2006).
[21] M. K. Petersen, A. J. Hatt, and G. A. Voth, J. Phys. Chem. B **112**, 7754 (2008).
[22] O. Borodin and G. D. Smith, Macromolecules **33**, 2273 (2000).
[23] J. K. Hyun, H. T. Dong, C. P. Rhodes, R. Frech, and R. A. Wheeler, J. Phys. Chem. B **105**, 3329 (2001).
[24] C. Do, P. Lunkenheimer, D. Diddens, M. Gotz, M. Weiss, A. Loidl, X. G. Sun, J. Allgaier, and M. Ohl, Phys. Rev. Lett. **111**, 018301 (2013).
[25] F. L. Tanzella, W. Bailey, D. Frydrych, G. C. Farrington, and H. S. Story, Solid State Ionics **5**, 681 (1981).
[26] S. A. Hashmi, J. Mater. Sci. **33**, 989 (1998).
[27] Z. Tao and P. T. Cummings, Mol. Simul. **33**, 1255 (2007).
[28] R. Langer and D. A. Tirrell, Nature (London) **428**, 487 (2004).
[29] R. Langer, Nature (London) **392**, 5 (1998).
[30] R. Langer, Science **293**, 58 (2001).
[31] T. L. Krause and G. D. Bittner, Proc. Natl. Acad. Sci. U.S.A. **87**, 1471 (1990).
[32] S. H. Chen, L. Liu, E. Fratini, P. Baglioni, A. Faraone, and E. Mamontov, Proc. Natl. Acad. Sci. U.S.A. **103**, 9012 (2006).
[33] R. Bergman and J. Swenson, Nature (London) **403**, 283 (2000).
[34] A. Kalra, S. Garde, and G. Hummer, Proc. Natl. Acad. Sci. U.S.A. **100**, 10175 (2003).
[35] L. Hong, D. C. Glass, J. D. Nickels, S. Perticaroli, Z. Yi, T. Madhusudan, H. O'Neill, Q. Zhang, A. P. Sokolov, and J. C. Smith, Phys. Rev. Lett. **110**, 028104 (2013).
[36] L. Hong, N. Smolin, and J. C. Smith, Phys. Rev. Lett. **112**, 158102 (2014).
[37] See Supplemental Material for detailed methods and analysis for both experiments and simulations at http://link.aps.org/supplemental/10.1103/PhysRevLett.115.198301, which includes Refs. [12,38–57].
[38] E. Mamontov and K. W. Herwig, Rev. Sci. Instrum. **82**, 085109 (2011).
[39] H. Bekker, H. J. C. Berendsen, E. J. Dijkstra, S. Achterop, R. Vondrumen, D. Vanderspoel, A. Sijbers, H. Keegstra, B. Reitsma, and M. K. R. Renardus, Phys. Comp. **92**, 252 (1993).
[40] D. Van Der Spoel, E. Lindahl, B. Hess, G. Groenhof, A. E. Mark, and H. J. Berendsen, J. Comput. Chem. **26**, 1701 (2005).
[41] B. Hess, C. Kutzner, D. van der Spoel, and E. Lindahl, J. Chem. Theory Comput. **4**, 435 (2008).
[42] W. L. Jorgensen and J. Tiradorives, J. Am. Chem. Soc. **110**, 1657 (1988).
[43] W. L. Jorgensen, D. S. Maxwell, and J. TiradoRives, J. Am. Chem. Soc. **118**, 11225 (1996).

[44] G. Bussi, D. Donadio, and M. Parrinello, J. Chem. Phys. **126**, 014101 (2007).
[45] S. Melchionna, Phys. Rev. E **61**, 6165 (2000).
[46] A. C. Barnes, T. W. N. Bieze, J. E. Enderby, and J. C. Leyte, J. Phys. Chem. **98**, 11527 (1994).
[47] B. Wu, Y. Liu, X. Li, E. Mamontov, A. I. Kolesnikov, S. O. Diallo, C. Do, L. Porcar, K. L. Hong, S. C. Smith *et al.*, J. Am. Chem. Soc. **135**, 5111 (2013).
[48] B. Wu, B. Kerkeni, T. Egami, C. Do, Y. Liu, Y. M. Wang, L. Porcar, K. L. Hong, S. C. Smith, E. L. Liu *et al.*, J. Chem. Phys. **136**, 144901 (2012).
[49] S. Dixit, J. Crain, W. C. Poon, J. L. Finney, and A. K. Soper, Nature (London) **416**, 829 (2002).
[50] Y. Ding, A. A. Hassanali, and M. Parrinello, Proc. Natl. Acad. Sci. U.S.A. **111**, 3310 (2014).
[51] T. Rog, K. Murzyn, K. Hinsen, and G. R. Kneller, J. Comput. Chem. **24**, 657 (2003).
[52] B. J. Drouin, S. S. Yu, J. C. Pearson, and H. Gupta, J. Mol. Struct. **1006**, 2 (2011).
[53] E. Mamontov, Chem. Phys. Lett. **530**, 55 (2012).
[54] S. Mitra, R. Mukhopadhyay, I. Tsukushi, and S. Ikeda, J. Phys. Condens. Matter **13**, 8455 (2001).
[55] O. Borodin, F. Trouw, D. Bedrov, and G. D. Smith, J. Phys. Chem. B **106**, 5184 (2002).
[56] S. B. Rempe, L. R. Pratt, G. Hummer, J. D. Kress, R. L. Martin, and A. Redondo, J. Am. Chem. Soc. **122**, 966 (2000).
[57] G. Stirnemann, E. Wernersson, P. Jungwirth, and D. Laage, J. Am. Chem. Soc. **135**, 11824 (2013).
[58] S. Cerveny, G. A. Schwartz, R. Bergman, and J. Swenson, Phys. Rev. Lett. **93**, 245702 (2004).
[59] S. Cerveny, A. Alegria, and J. Colmenero, Phys. Rev. E **77**, 031803 (2008).
[60] J. Swenson and S. Cerveny, J. Phys. Condens. Matter **27**, 033102 (2015).
[61] M. Rosenstihl, K. Kampf, F. Klameth, M. Sattig, and M. Vogel, J. Non-Cryst. Solids **407**, 449 (2015).
[62] S. Khodadadi, S. Pawlus, and A. P. Sokolov, J. Phys. Chem. B **112**, 14273 (2008).
[63] G. D. Smith and D. Bedrov, J. Polym. Sci., Part B: Polym. Phys. **45**, 627 (2007).
[64] O. Borodin, D. Bedrov, and G. D. Smith, J. Phys. Chem. B **106**, 5194 (2002).
[65] Q. Liu, R. K. Schmidt, B. Teo, P. A. Karplus, and J. W. Brady, J. Am. Chem. Soc. **119**, 7851 (1997).
[66] W. L. Jorgensen and C. Jenson, J. Comput. Chem. **19**, 1179 (1998).
[67] P. E. Smith, H. D. Blatt, and B. M. Pettitt, J. Phys. Chem. B **101**, 3886 (1997).
[68] M. Holz, S. R. Heil, and A. Sacco, Phys. Chem. Chem. Phys. **2**, 4740 (2000).
[69] E. Guarini, M. Sampoli, G. Venturi, U. Bafile, and F. Barocchi, Phys. Rev. Lett. **99**, 167801 (2007).
[70] P. R. Chinnam and S. L. Wunder, J. Mater. Chem. A **1**, 1731 (2013).
[71] J. M. Tarascon and M. Armand, Nature (London) **414**, 359 (2001).
[72] S. E. Kim, I. B. Lee, C. Hyeon, and S. C. Hong, J. Phys. Chem. B **118**, 4753 (2014).
[73] A. V. Egorov, A. V. Komolkin, V. I. Chizhik, P. V. Yushmanov, A. P. Lyubartsev, and A. Laaksonen, J. Phys. Chem. B **107**, 3234 (2003).